Remote Sensing of Environment 114 (2010) 693–699

Contents lists available at ScienceDirect

Remote Sensing of Environment

journal homepage: www.elsevier.com/locate/rse

Sea ice surface features in Arctic summer 2008: Aerial observations

Peng Lu [a,*], Zhijun Li [a], Bin Cheng [a,b], Ruibo Lei [a], Rui Zhang [a]

[a] State Key Laboratory of Coastal and Offshore Engineering, Dalian University of Technology, Dalian, China
[b] Finnish Meteorological Institute, Helsinki, Finland

ARTICLE INFO

Article history:
Received 28 May 2009
Received in revised form 11 November 2009
Accepted 16 November 2009

Keywords:
Arctic
Sea ice
Aerial photography
AMSR-E
Melt pond

ABSTRACT

Eight helicopter flights were conducted, and more than 9000 aerial images were obtained during the Third Chinese National Arctic Research Expedition in 2008 in the Pacific Arctic Sector (PAS). Along the cruise tracks between 77°N and 86°N, area fractions of open water and ice cover varied from 0.96 to 0.12 and from 0.03 to 0.81, respectively, while the melt pond fraction varied between 0 and 0.2. The ice concentrations derived from aerial images and the AMSR-E/ASI products were comparable to each other, especially in the range of 50–90%. However, the satellite-derived data overestimated the aerial observations by $14 \pm 9\%$ in areas with large ice concentrations (>90%), and nearly ignored those with very low ice concentrations (<20%). In addition, a significantly higher amount of melt ponds was observed in the PAS in the summer of 2008 as compared to five years ago. The areally averaged albedo increased from 0.09 in the marginal ice zone at 77°N to 0.63 in the far north zone at 86°N, where the ice concentration was 90%. The albedo was significantly smaller than those reported in earlier studies in the PAS for the same region because of an overall decrease in ice concentration. Compared with 2007 data, the lower ice concentration in 2008 may yield a smaller total ice-covered area, although the Arctic ice extent in 2008 was slightly larger than the record minimum in 2007.

1. Introduction

The extent of Arctic sea ice reached its minimum in history in September 2007, measuring only 4.1×10^6 km^2 (Comiso et al., 2008). The second lowest measurement was recorded in September 2008, totaling only 4.5×10^6 km^2, according to the National Snow and Ice Data Center (NSIDC) (http://nsidc.org/arcticseaicenews). The importance of Arctic sea ice in the global climate has been well demonstrated (e.g., Francis et al., 2009). In addition, various studies have been conducted to identify the causes of ice retreat (Zhang et al., 2008; Wang et al., 2009). The projected Arctic sea ice extent has been estimated using Intergovernmental Panel on Climate Change (IPCC) models (Wang & Overland, 2009), which have indicated that there may be a sea ice-free Arctic summer within 30 years. Numerical models and satellite remote sensing are crucial to understanding Arctic sea ice patterns. However, few or no model simulations can produce trends comparable to actual observations. Models evaluating the future evolution of Arctic sea ice cover during the 21st century also show a large scatter between predictions (Stroeve et al., 2007). Accordingly, there is a strong need for a better understanding of many important physical processes involved in changes of Arctic sea ice, such as the role that the ice-albedo feedback mechanism plays in coping with the loss of Arctic sea ice.

Satellite remote sensing is a powerful tool for the large-scale assessment of Arctic sea ice cover (e.g., Drobot, 2007; Tschudi et al., 2008). It is well known that the sequence of changes in the extent of Arctic sea ice has been detected since reliable satellite measurements became available in 1979. Sea ice concentration, for instance, has been retrieved by passive microwave sensors since the application of the Electrically Scanning Microwave Radiometer (ESMR) sensor in 1972. Since 1987, the Special Sensor Microwave/Imager (SSM/I) has been widely used for sea ice concentration determination. In 2002, a new sensor, Advanced Microwave Scanning Radiometer for the Earth Observing System (AMSR-E), on the AQUA platform became available. The main advantage of this new sensor over others used before is its improved horizontal resolution. AMSR-E offers spatial resolutions of approximately 6 km × 4 km at 89 GHz, nearly three times the resolution of SSM/I at 85 GHz (15 km × 13 km). Moreover, the Arctic Radiation and Turbulence Interaction Study Sea Ice (ASI) algorithm based on 89 GHz data enables the daily estimation of sea ice concentration in a 6.25 km grid, which is up to four times finer than the resolution of other algorithms, such as the NASA Team or Bootstrap, which use lower-frequency channels (Spreen et al., 2008).

However, the usefulness of satellite instruments is always limited by certain preconditions. For example, operational passive microwave sensors are limited by their coarse spatial resolution from distinguishing open water from ponded ice, and the optical sensors are severely restricted by a persistent cloud cover over ice packs from detecting melt ponds (Inoue et al., 2008). The usage of AMSR-E at 89 GHz channels is also limited by the considerably higher atmospheric

* Corresponding author. Tel.: +86 411 8470 8271; fax: +86 411 8470 8526.
E-mail address: lupeng@dlut.edu.cn (P. Lu).

0034-4257/$ – see front matter © 2009 Elsevier Inc. All rights reserved.
doi:10.1016/j.rse.2009.11.009

influence from water vapor and clouds than lower-frequency channels (Spreen et al., 2008). Accordingly, in situ observation of Arctic sea ice is important and necessary to validate existing remote sensing algorithms and numerical models (e.g., Hall et al., 2008; Connor et al., 2009). Aerial photography surveys have long been an effective method of understanding the spatial variability in sea ice with a higher resolution that is difficult or impossible to obtain remotely. As a result, this method has been widely used in field expeditions to provide ground truth on sea ice for further comparisons and analyses (e.g., Markus et al., 2003; Perovich et al., 2009).

In this study, we evaluated aerial photographs that were obtained in summer during the Third Chinese National Arctic Research Expedition in 2008 (CHINARE2008). The spatial variability of open water, melt pond, and ice cover in the Pacific Arctic Sector (PAS) was determined. In addition, we determined ice concentration based on aerial images, and compared it with that derived from satellite microwave observations of AMSR-E using the 89 GHz ASI algorithm. The areally averaged surface albedo was then calculated and compared with other measurements conducted in the PAS in previous studies.

2. Field investigation

CHINARE2008 is a part of the International Polar Year (IPY) China Program, which was conducted from 11 July until 25 September 2008. The Chinese Research Vessel Xuelong from the Polar Research Institute of China was used as the expedition platform. The PAS (including the Bering Sea, Bering Strait, Chukchi Sea, Beaufort Sea, and Canada Basin) is the primary investigation area for CHINARE2008, where sea ice retreats faster than in other regions of the Arctic (Nghiem et al., 2007). Sea ice in the PAS also underwent a rapid retreat in the summer of 2008. From 6 August to 5 September 2008, R/V Xuelong was cruising in this area and witnessed the processes. The edge of the marginal ice zone (MIZ) was observed at approximately 76°N on 13 August when the ship sailed northward. When the ship returned on 4 September, MIZ had retreated to 78°N. A total of eight helicopter flights were conducted to perform an aerial survey of sea ice distributions during CHINARE2008. The flight routes and ship tracks are shown in Fig. 1.

To conduct the aerial surveys, an iron box was mounted outside the helicopter in a downward-facing orientation. The box contained a Canon G9 camera, a portable GPS, and a pressure differential altimeter. A data cable was used to connect the camera to a laptop computer onboard the helicopter. The camera had a resolution of 3264×2248 pixels. The flight altitude varied according to weather conditions, but was generally around 100 m. At this height, each snap shot covered an area of approximately 98 m × 67 m, yielding a resolution of 0.03 m per pixel. The images were spaced without overlapping, and each image represented an independent scene. The total time for all flights was 1180 min, and 9584 images were collected. Only 2% of images could not be processed because of the poor contrast resulting from low clouds or fog. The images covered the locations 77.0°N–86.5°N and 143.2°W–180.0°W.

3. Aerial image processing

During the flight surveys, sea ice was undergoing a transition period from the late melting phase to the early freeze-up phase. Snow was largely seen on top of the ice. The surface characteristics were partitioned into three components: snow-covered ice floe, melt ponds, and open leads. Each fraction was detected based on differences in the brightness and color of the images. The fractional areas were presented as A_{si} (snow-covered ice), A_p (pond), and A_w (water). For each unit area, $A_{si} + A_p + A_w = 1$. Ice concentration is the sum of A_{si} and A_p.

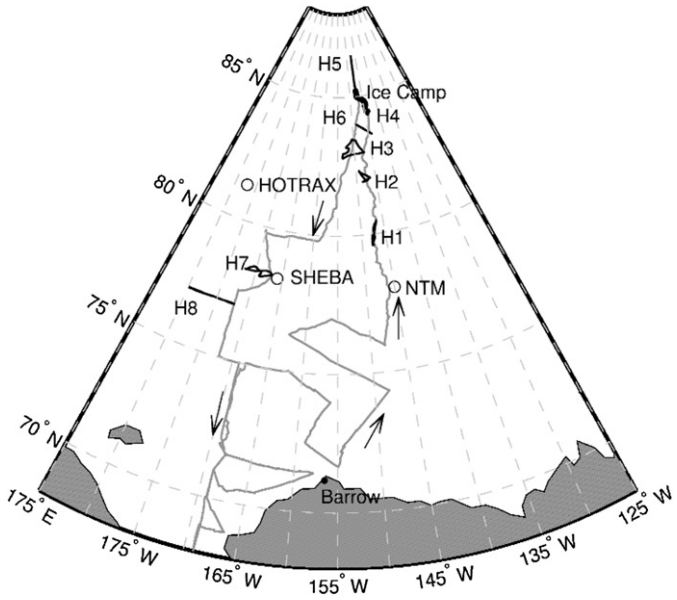

Fig. 1. The CHINARE2008 cruise track (gray) and eight (H1 to H8) helicopter flight trajectories (black). The black arrows indicate the cruise direction. The flights were conducted daily from 17 to 20 August (H1–H4), 30 to 31 August (H5–H6), and 4 to 5 September (H7–H8) 2008. The thick solid segment shows the Ice Camp drift trajectory from 20 to 29 August. Circles refer to several other field campaigns in which aerial images were obtained and compared with our results (see text for details regarding the campaigns).

Partitioning of the image into three-category surface fractions was executed by manually selecting red, green, and blue (RGB) thresholds based on color distribution histograms (Perovich et al., 2002a; Inoue et al., 2008). Color was useful in identifying the melt ponds from the surrounding pack ice because they typically look bluish, and the albedo of ponds is substantially lower than that of pack ice. In addition, pond reflectance is greater in the blue portion of the spectrum than in the red (Grenfell & Maykut, 1977) as compared to the relatively flat spectral signature of the surrounding ice. Open water can also be identified by using its low reflectance to separate it from first-year and multiyear ice, and its flat spectral return to distinguish it from ponds. Thus, the threshold levels for each surface category in each image were independently determined.

Some special conditions must be specified: pond-like features (edge erosion) typically resulting from lateral melting presented for some ice floes. In our analysis, these features were characterized as melt ponds because their optical characteristics were similar to those of ponds on ice. Melt ponds that penetrated through (i.e., melt holes) were optically similar to leads due to the same RGB distributions; therefore, they were classified as open water. These melt holes were essentially equivalent to leads in physical terms, so those treated as open water in the classification algorithm were warranted. In later flights, thin young ice occasionally appeared in both leads and ponds. These layers were treated as ponds or leads because they were too thin to change the surface reflection. Approximately 30% of the total images contained no melt ponds, and were therefore classified into water and ice using a threshold segmentation procedure (Lu et al., 2008).

4. Results and discussions

4.1. General ice surface features

A qualitative knowledge of the sea ice conditions at different locations can be gleaned from visually inspecting the aerial images. When the first survey flight began on 17 August 2008, the sea ice was still under the summer melting phase. The mature melt ponds had formed distinct shapes, and the different hues of blue were associated